Proceedings of the Sixth International Conference on
Railway Technology: Research, Development and Maintenance
Edited by: J. Pombo
Civil-Comp Conferences, Volume 7, Paper 5.7
Civil-Comp Press, Edinburgh, United Kingdom, 2024
ISSN: 2753-3239, doi: 10.4203/ccc.7.5.7

Improving Ride Comfort of Railway Vehicles on High-Speed Tracks Using Model Predictive Control

A. Posseckert

Institute of System Dynamics and Control, German Aerospace Center (DLR), Oberpfaffenhofen, Germany

Abstract

This paper introduces a control strategy for active secondary suspension based on Model Predictive Control. The influence of the track irregularities and track layout upon carbody lateral and vertical dynamics is considered explicitly. The developed controller is applied to a full-scale rail vehicle model. Ride comfort is evaluated according to EN 12299. Multibody simulations show that on a realistic high-speed track there is a significant increase of ride comfort.

Keywords: railway vehicle, ride comfort, active secondary suspension, model predictive control, preview, active suspension

1 Introduction

Railway transport will play an even more important role in future mobility due to its environmental friendliness. A recently published study presented by Deutsche Bahn proposes a 'Metropolitan Network' [1] which connects all large cities in Europe to the high-speed rail network with service at least once an hour. The study refers to EU Commission's Green Deal that intends to double high-speed rail traffic 2030 and

a triple it by 2050. A key aspect for success is the competitiveness with flight traffic, therefore a high travel speed up to $300\,\mathrm{km\,h^{-1}}$ is planned [1].

Another essential issue to increase the attractiveness of railway transport is to provide a good ride comfort in all situations. In the current rail network, most of the ordinary railway vehicles with conventional suspension systems already provide sufficient ride comfort [2]. However, when driving at higher speeds on existing tracks without increasing track quality, this might not be the case anymore.

1.1 State of the art

A good option to increase ride comfort is the usage of active or semi-active components in the secondary suspension. A general overview regarding this research topic is given in [2]. For example, tilting trains have become a great success in some countries [3]. Another low bandwidth application is the hold-off-device which prevents comfort-reducing bumpstop contact in the secondary suspension [4]. Commonly used regulators for controlling the secondary suspension are skyhook-damping [5], H∞ control [6] and combinations of them, respectively.

Another promising control strategy related to active suspension is model predictive control (MPC). One of its advantages is the ability to handle constraints, e.g. restrict suspension deflections. Furthermore, the ability to directly consider future disturbances (e.g. the track ahead) can be included. While widespread in automotive research, MPC is not commonly used for active suspension in railway technology. For example, a MPC-based approach is implemented in [7] where acceleration as well as suspension deflection can be successfully reduced. However, the study only focusses on vertical dynamics, such as bouncing and pitching. A recent work shows that on poor-quality tracks a significant increase of lateral ride comfort can be achieved [8].

To fully exploit its potential, MPC requires modern communication channels in order to determine the current train position or for data exchange between train and infrastructure. Some of today's rail traffic management systems are based on the old-fashioned Global System for Mobile Communications-Railway (GSM-R) standard. The successor of it is the Future Railway Mobile Communication System (FRMCS) which already lists the provision of the train's current location as possible critical support application [9]. This shows that FRMCS could be an enabler for new applications in the field of active suspension. However, the previously mentioned conventional controllers like skyhook-damping do not take advantage of this, which means that the potential of modern railway communication technologies is still underexplored.

1.2 Goals and structure of the work

In this regard, the goal of this work is to outline a control strategy for active secondary suspension which takes advantage of the connectivity between the train and infrastructure. The regulator is based on MPC due to the ability to anticipate and compensate for future disturbances that impact the railway vehicle. The focus is on how the

knowledge of the track ahead including measured track irregularities can be used in order to increase ride comfort. The proposed control strategy is applied to multibody simulations of the Next Generation Train (NGT). In this project German Aerospace Center (DLR) is investigating what future high-speed trains could look like [10, 11]. Ride comfort is evaluated according to EN 12299 [12]. To emphasize the differences comparative simulations are carried out using conventional secondary suspension.

Section 2 introduces the analytical model of the vehicle and the controller which takes the model as input. The simulation environment and results are presented in Section 3, followed by a short summary in Section 4.

2 Modeling and controller design

The following degrees of freedom (DOF) are considered for the carbody, see Figure 1: Lateral displacement y_{cb}, vertical displacement z_{cb}, roll angle ϕ_{cb}, yaw angle ψ_{cb} and pitch angle γ_{cb}. In addition, each bogie has a translational DOF in vertical direction $z_{bg,fr/re}$. Rotational movement around x-axis by the angle $\phi_{bg,fr/re}$ is also allowed. This yields a model with 9 DOF, see Equation (1).

$$\vec{q} = \begin{bmatrix} y_{cb} & z_{cb} & \phi_{cb} & \gamma_{cb} & \psi_{cb} & z_{bg,fr} & \phi_{bg,fr} & z_{bg,re} & \phi_{bg,re} \end{bmatrix}^T \tag{1}$$

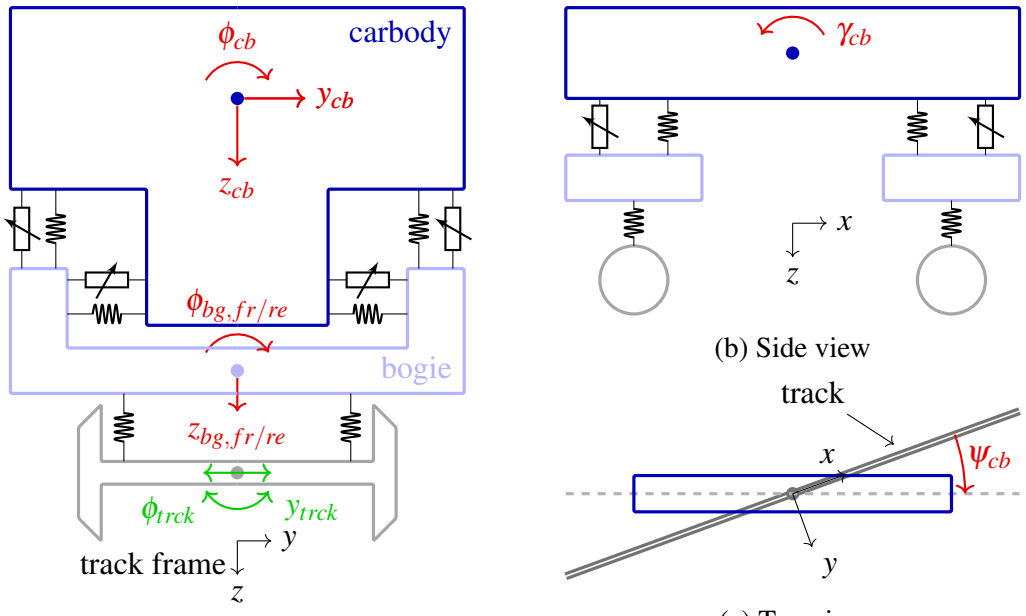

(a) Cross section

(b) Side view

(c) Top view

Figure 1: Definition degrees of freedom (red). Furthermore, the base excitation of both front and rear axle bridge due to track irregularities (green) is shown.

2.1 Influence of the track upon carbody dynamics

During the process of creating the analytical model, the influence of track irregularities as well as track layout is considered explicitly, which is explained further below. First, track errors are taken into account by modelling them as base excitation of the axle bridge. For lateral dynamics this has been already described in [8] and is therefore only briefly summarized below.

The running gear design of the NGT includes driven independently rotating wheels. Therefore, lateral guidance control is required in order to perform active steering of the wheels, see [13]. The controller designed for this purpose significantly influences the axle bridge movement and, thus, the impact of track errors upon carbody dynamics. In order to simplify this complex closed-loop behavior when creating the model, it is proposed to approximate the resulting dynamics of the axle bridge by a transfer function. Figure 2 illustrates the response of the axle bride to a (non-unitary) step function for lateral displacement. It is found that a transfer function with a numerator degree of 1 and denominator degree of 2, as given in Equation (2), is sufficient to approximate the illustrated response. The result was obtained from a multibody simulation of the NGT at a velocity of $300\,\mathrm{km\,h^{-1}}$. In general, the response depends on velocity. To conclude, the axle bridge of the analytical model is excited by track irregularities which have been filtered through a velocity dependent transfer function.

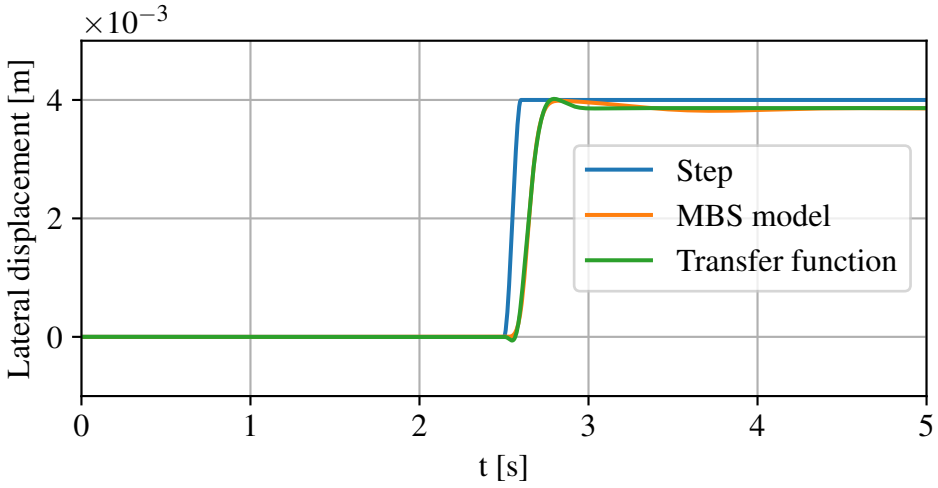

Figure 2: Step response of the guidance controller and the transfer function

$$TF_{300} = \frac{-8.021\,s + 381.6}{s^2 + 28.25\,s + 395.2}. \tag{2}$$

The components of track excitation at both front and rear bogie are collected in the disturbance vectors $\vec{z}_1$ and $\vec{z}_2$, see Equation (3).

$$\begin{aligned} \vec{z}_1 &= \begin{bmatrix} y_{trck,fr} & y_{trck,re} & z_{trck,fr} & z_{trck,re} & \phi_{trck,fr} & \phi_{trck,re} \end{bmatrix}^T \\ \vec{z}_2 &= \begin{bmatrix} \dot{y}_{trck,fr} & \dot{y}_{trck,re} & \dot{z}_{trck,fr} & \dot{z}_{trck,re} & \dot{\phi}_{trck,fr} & \dot{\phi}_{trck,re} \end{bmatrix}^T \end{aligned} \tag{3}$$

As mentioned above, besides irregularities the influence of track characteristics is considered as well. On scenarios like track changes when entering or leaving a station this has already been described in [14]. For tracks with superelevation a more general approach is needed. To achieve this, the equations of motion are derived relative to a non-inertial track frame that follows the track at top of rail, see Figure 1. The longitudinal position of the frame along the track as well as its current velocity coincide with carbody's center of gravity. Potentially occurring superelevation is also taken into account.

As a result, fictitious forces have to be considered. According to [15] the general formulation of Newton's second law in a non-inertial frame can be written as

$$\begin{aligned} m\,\vec{a}' &= \vec{F}_{External} - m\,\vec{\omega}\times\vec{r}' - 2m\,\vec{\omega}\times\vec{v}' - m\,\vec{\omega}\times(\vec{\omega}\times\vec{r}') - m\,\ddot{\vec{R}} \\ &= \vec{F}_{External} + \vec{F}_{Euler} + \vec{F}_{Coriolis} + \vec{F}_{Centrifugal} + \vec{F}_{Frame}. \end{aligned} \tag{4}$$

The prime $'$ denotes quantities measured w.r.t. track frame. Euler force acts on the carbody when there is an abrupt change of superelevation hence when its time derivative is not constant. The lateral component is

$$F_{Euler,lat} = -m_{cb}\,\dot{\omega}_x\,a_{cog} \tag{5}$$

where $\dot{\omega}_x$ is the second time-derivative of the current superelevation. The vertical distance between track frame and carbody's center of gravity is described by a_{cog}. The influence of Coriolis force is neglected since carbody's velocity relative to track frame is small. Due to the position of the track frame below the carbody (and not in the center of curvature), centrifugal force is not taken into account as well.

Forces described by $\vec{F}_{Frame}$ occur due to the acceleration of the track frame origin measured w.r.t. inertial frame of reference. The weight of the carbody is included in $\vec{F}_{External}$. For deriving the equations of motion, it is useful to extract the component of the latter two forces that act on the carbody in lateral direction (which might not be horizontal due to superelevation). This is done as follows.

$$F_{lat,cb} = -m_{cb}\,\frac{cd}{153} \tag{6}$$

where the current cant deficiency is denoted by cd, which in turn is based on vehicle speed, track curvature and the current superelevation. Of course both bogies are affected by ficticious forces as well. However, since the carbody mass is considerably higher compared to the bogies, no major influence is expected. The previously mentioned forces are now collected in the disturbance vector $\vec{z}_3$

$$\vec{z}_3 = \begin{bmatrix} F_{Euler,lat} & F_{lat,cb} \end{bmatrix}^T \tag{7}$$

which in turn is collected in a large vector $\vec{z}$

$$\vec{z} = \begin{bmatrix} \vec{z}_1 & \vec{z}_2 & \vec{z}_3 \end{bmatrix}^T \tag{8}$$

While deriving the equations of motion via Newton–Euler, the following additional assumptions are made:

- Due to the mechatronic guidance of NGT's running gear, flange contact does not occur.
- Bumpstop contact can be avoided since MPC has the ability to handle state restrictions (e.g., suspension deflections).
- Small angles of roll, pitch and yaw are assumed.

Based on these assumptions, the equations of motion can be linearized. A detailed description is given in Appendix A.1.

$$\vec{M}\,\ddot{\vec{q}} + \vec{D}\,\dot{\vec{q}} + \vec{K}\,\vec{q} = \vec{F}_{act}\,\vec{u} + \vec{F}_{dist}\,\vec{z}. \tag{9}$$

Subsequently, the system is transformed into state space form

$$\begin{aligned} \dot{\vec{x}} &= \vec{A}\,\vec{x} + \vec{B}\,\vec{u} + \vec{E}\,\vec{z} \\ \vec{y} &= \vec{C}\,\vec{x} \end{aligned} \tag{10}$$

with

$$\vec{x} = \begin{bmatrix} \vec{q} & \dot{\vec{q}} \end{bmatrix}^T \tag{11}$$

In the secondary suspension, the actuators are mounted in both lateral and vertical directions, see Figure 1. Consequently, forces can be applied in the lateral and vertical direction as well as torques around the x, y and z-axis

$$\vec{u} = \begin{bmatrix} F_{lat} & F_{vert} & M_{roll} & M_{pitch} & M_{yaw} \end{bmatrix}^T \tag{12}$$

The carbody DOF are chosen as output

$$\vec{y} = \begin{bmatrix} y_{cb} & z_{cb} & \phi_{cb} & \gamma_{cb} & \psi_{cb} \end{bmatrix}^T \tag{13}$$

2.2 Model Predictive Control

Equation (10) is now transformed to discrete formulation with timestep k using the zero-order hold method. Furthermore, control variable $\vec{u}$ can be written via its change in one timestep and its previous value; see Equation (14). Both formulations are equivalent, though it is easier to incorporate actuator dynamics later by restricting the change in each timestep

$$\vec{u}(k) = \vec{u}(k-1) + \Delta\vec{u}(k). \tag{14}$$

Finally, one obtains

$$\begin{aligned} \vec{x}(k+1) &= \vec{A}_d\,\vec{x}(k) + \vec{B}_d\,\vec{u}(k-1) + \vec{B}_d\,\Delta\vec{u}(k) + \vec{E}_d\,\vec{z}(k) \\ \vec{y}(k) &= \vec{C}_d\,\vec{x}(k) \end{aligned} \tag{15}$$

Using the model described in Equation (15), MPC minimizes a cost function J over the prediction horizon n_p by determining an optimal sequence of control variables over

the control horizon n_c. The optimization problem is solved using a QP-solver [16]. Then, the first element of the sequence is applied and the process is repeated in the next timestep $k+1$, see [17]. When setting up the cost function, system output, control variables and disturbances are collected in a single vector for the whole prediction horizon and control horizon, respectively, see Equation (16).

$$\bar{\vec{y}}(k+1) = \begin{bmatrix} \vec{y}(k+1) \\ \vec{y}(k+2) \\ \vdots \\ \vec{y}(k+n_p) \end{bmatrix}, \; \Delta\bar{\vec{u}}(k) = \begin{bmatrix} \Delta\vec{u}(k) \\ \Delta\vec{u}(k+1) \\ \vdots \\ \Delta\vec{u}(k+n_c-1) \end{bmatrix}, \; \bar{\vec{z}}(k) = \begin{bmatrix} \vec{z}(k) \\ \vec{z}(k+1) \\ \vdots \\ \vec{z}(k+n_p-1) \end{bmatrix} \tag{16}$$

The output prediction over the prediction horizon is given by

$$\bar{\vec{y}}(k+1) = \vec{F}\,\vec{x}(k) + \vec{G}\,\vec{u}(k-1) + \vec{S}\bar{\vec{z}}(k) + \vec{H}\Delta\bar{\vec{u}}(k), \tag{17}$$

where $\vec{F}$, $\vec{G}$, $\vec{S}$ and $\vec{H}$ can be derived from the system matrices, as already explained in [8]. With weighting matrices $\vec{Q}$ and $\vec{R}$, the cost function J that has to be minimized can be formulated as

$$\begin{aligned} \min_{\Delta\bar{\vec{u}}(k)} \quad & J = \bar{\vec{y}}(k+1)^T \vec{Q}\,\bar{\vec{y}}(k+1) + \Delta\bar{\vec{u}}(k)^T \vec{R}\,\Delta\bar{\vec{u}}(k) \\ \text{s.t.} \quad & \Delta\vec{u}_{min} \le \Delta\vec{u}(k) \le \Delta\vec{u}_{max} \\ & \vec{y}_{min} \le \vec{y}(k) \le \vec{y}_{max}. \end{aligned} \tag{18}$$

3 Simulation environment and results

The controller derived in section 2.2 is applied to a full-scale vehicle model of an NGT coach. Due to some features of its carbody (single-wheelset bogies, lightweight design, doubledeck configuration) it turned out to be difficult to achieve a good ride comfort with exclusively passive suspension components. Therefore, the vehicle offers an ideal platform for testing the controller. The simulation consists of two parts. Multibody simulations are carried out in the *Simpack* software. For the controller, the built-in MPC toolbox of *Matlab/Simulink* is used. Both software products are interconnected using the co-simulation interface *Simat*.

3.1 Track scenario

A section of the high-speed track between Nuremberg and Ingolstadt, Germany, is selected as test route, see Figure 3. Regarding track geometric quality, the measured standard deviation of lateral alignment Δy_σ^0 is 0.48 mm, that of longitudinal level Δz_σ^0 is 0.35 mm. Both values are measured at the right rail, the left one has smaller track errors. Consequently, at a speed of 300 km h^{-1}, both values lie within or are even better than the target range TL90 according to EN 14363 [18], see Table 1.

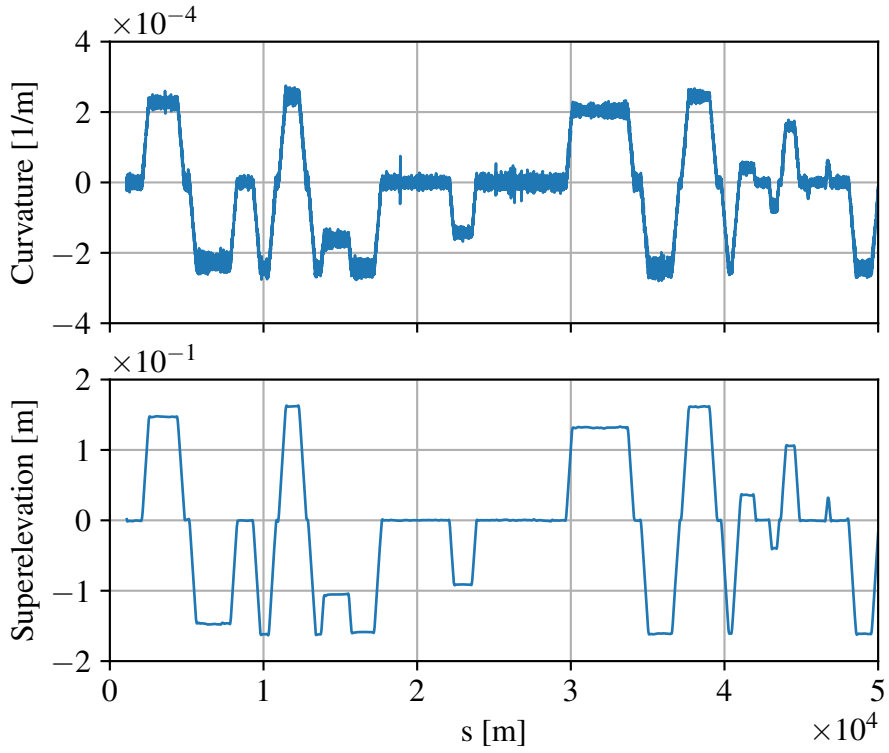

Figure 3: Properties of the track scenario

Reference Speed	**Alignment** Δy_σ^0	**Longitudinal Level** Δz_σ^0
$230 < V \leq 300\,\mathrm{km\,h^{-1}}$	0.50–0.65 mm	0.85–1.15 mm

Table 1: Track geometric quality: Target test ranges for standard deviation TL90 [18]

The evaluation of ride comfort is carried out according to EN 12299 [12]. This means the N_{MV}-value is determined, which incorporates longitudinal, lateral and vertical acceleration measured at several positions on both floors of the carbody, see Figure 4.

3.2 Results

Numerical results are presented in Figure 5. For comparison purposes the same simulation is carried out using a model of the NGT with purely passive secondary suspension. Using the control strategy proposed in Section 2.2 a better ride comfort can be reached at all points that are measured, recognizable by a lower N_{MV} value. For example, on the top floor at rear sensor position there is an improvement of 40% compared to the passive case. On both floors, ride comfort is better in the middle than at the front and rear of the carbody. When comparing the lower and upper floor it is noticeable that on the latter ride comfort is slightly better.

In order to fully exploit the potential of MPC, the current train location is required.

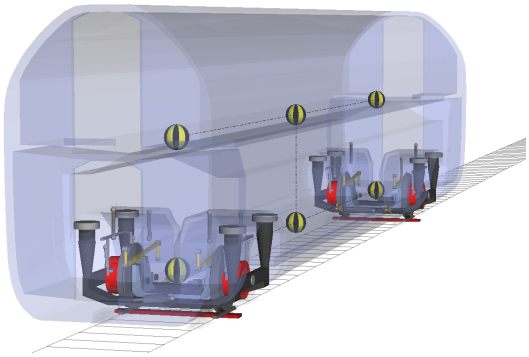

Figure 4: NGT coach with measurement points visualized as yellow spheres.

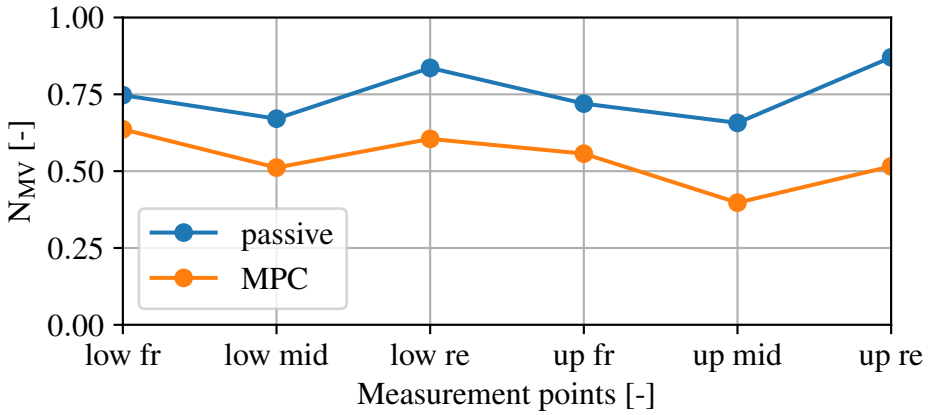

Figure 5: Ride comfort index evaluated at different measurement points

To obtain information regarding the required accuracy, several simulations are carried out in which white noise is superimposed on the positioning signal. The results are given in Table 2. Ride comfort obtained at the middle of the upper floor is given for different power spectral densities (PSD) of the added noise. Furthermore, the result of a simulation with passive secondary suspension is listed as well. The far-right column compares test cases with noisy localization to the reference case without errors. For example, it can be observed that ride comfort deteriorates by 25% if the PSD of the added noise is $5\,\mathrm{W\,Hz^{-1}}$. The variance of this signal is $5\,\mathrm{m^2}$.

PSD of noise	**Variance**	**NMV up re**	**Deterioration**
$5\,\mathrm{W\,Hz^{-1}}$	$5\,\mathrm{m^2}$	0.65	25%
$1\,\mathrm{W\,Hz^{-1}}$	$1\,\mathrm{m^2}$	0.59	13%
-	-	0.52	0%
passive	-	0.87	68%

Table 2: Comfort index depending on the PSD of the superimposed white noise

3.3 Discussion

The results obtained in Section 3.2 show that the model given in Equation (15) is suitable for predicting carbody dynamics to track irregularities and track layout, respectively. Using MPC, it is shown that a significant increase in ride comfort can be achieved compared to a model with passive secondary suspension, see Figure 5. In addition, slightly better N_{MV} values are obtained on the upper floor compared to the lower floor. This indicates that the roll motion of the carbody is suppressed effectively.

Furthermore, the influence of stochastic positioning errors on ride comfort is investigated, see Table 2. A variance of up to $5\,m^2$ still enables significant improvements compared to a vehicle with passive secondary suspension. However, beside stochastic noise, a constant positioning error deteriorates controller performance as well, as already mentioned in [8]. This behaviour is plausible since the effect of a single bump upon carbody dynamics is tied to a very specific location. This represents a challenging requirement in terms of train localisation. However, for other applications like automatic train operation (which is already listed as possible critical communication application for FRMCS [9]), precise and reliable train position data is required as well. Therefore, it is likely that the required position accuracy needed for this application can be reached.

4 Conclusion

In this paper a control strategy for active secondary suspension based on Model Predictive Control (MPC) is introduced. Due to modern communication systems like FRMCS, the availability of data about the train and its environment is improving. This in turn can be used for new applications, e.g. active suspension that increases ride comfort by using information about the track ahead.

In order to design the controller, a model which describes carbody dynamics is developed. The impact of track irregularities and track layout is considered explicitly. The developed controller is applied to a multibody simulation of the NGT. A section of the high-speed track between Nuremberg and Ingolstadt, Germany, is selected as test scenario. On the selected tracks, there is a significant improvement of ride comfort at each measurement point.

To investigate the required positioning accuracy, simulations are carried out in which white noise is superimposed on the positioning signal. It was found that MPC still provides significant improvements when the PSD of the white noise is $5\,W\,Hz^{-1}$. Since other applications like automatic train operation require precise and reliable train position data as well, it is expected that this accuracy can be reached.

Multibody simulations of the NGT showed promising results. However, as mentioned in [8], this control strategy puts high requirements on the actuator dynamics. Therefore, the next step is to investigate the usage of semi-active components instead of active ones. The results of this paper can then be used as a reference.

A Appendix

A.1 System matrices

$$\vec{M} = \begin{bmatrix} 2.8\text{E}4 & 0 & 0 & 0 & 0 & 0 & 0 & 0 & 0 \\ 0 & 5.8\text{E}4 & 0 & 0 & 0 & 0 & 0 & 0 & 0 \\ 0 & 0 & 4.2\text{E}2 & 0 & 0 & 0 & 0 & 0 & 0 \\ 0 & 0 & 0 & 4.2\text{E}2 & 0 & 0 & 0 & 0 & 0 \\ 0 & 0 & 0 & 0 & 1.1\text{E}6 & 0 & 0 & 0 & 0 \\ 0 & 0 & 0 & 0 & 0 & 2.8\text{E}4 & 0 & 0 & 0 \\ 0 & 0 & 0 & 0 & 0 & 0 & 4.5\text{E}2 & 0 & 0 \\ 0 & 0 & 0 & 0 & 0 & 0 & 0 & 4.5\text{E}2 & 0 \\ 0 & 0 & 0 & 0 & 0 & 0 & 0 & 0 & 1.1\text{E}6 \end{bmatrix} \tag{19}$$

$$\vec{D} = \begin{bmatrix} 3.5\text{E}4 & -5.7\text{E}4 & 0 & 0 & 0 & 0 & 0 & 0 & 0 \\ -5.7\text{E}4 & 1.4\text{E}5 & -2.3\text{E}4 & -2.3\text{E}4 & 0 & 0 & 0 & 0 & 0 \\ 0 & -2.3\text{E}4 & 2.5\text{E}5 & 0 & 0 & 0 & 0 & 0 & 0 \\ 0 & -2.3\text{E}4 & 0 & 2.5\text{E}5 & 0 & 0 & 0 & 0 & 0 \\ 0 & 0 & 0 & 0 & 1.7\text{E}6 & 0 & 0 & 0 & 0 \\ 0 & 0 & 0 & 0 & 0 & 8\text{E}4 & -4\text{E}4 & -4\text{E}4 & 0 \\ 0 & 0 & 0 & 0 & 0 & -4\text{E}4 & 3.7\text{E}5 & 0 & 2.8\text{E}5 \\ 0 & 0 & 0 & 0 & 0 & -4\text{E}4 & 0 & 3.7\text{E}5 & -2.8\text{E}5 \\ 0 & 0 & 0 & 0 & 0 & 0 & 2.8\text{E}5 & -2.8\text{E}5 & 3.9\text{E}6 \end{bmatrix} \tag{20}$$

$$\vec{K} = \begin{bmatrix} 1.6\text{E}5 & -2.5\text{E}5 & -1.5\text{E}5 & -1.5\text{E}5 & 0 & 0 & 0 & 0 & 0 \\ -2.5\text{E}5 & 9\text{E}5 & -2.3\text{E}5 & -2.3\text{E}5 & 0 & 0 & 0 & 0 & 0 \\ -1.5\text{E}5 & -2.3\text{E}5 & 2.6\text{E}6 & 0 & -1.1\text{E}6 & 0 & 0 & 0 & 0 \\ -1.5\text{E}5 & -2.3\text{E}5 & 0 & 2.6\text{E}6 & 1.1\text{E}6 & 0 & 0 & 0 & 0 \\ 0 & 0 & -1.1\text{E}6 & 1.1\text{E}6 & 7.8\text{E}6 & 0 & 0 & 0 & 0 \\ 0 & 0 & 0 & 0 & 0 & 7.1\text{E}5 & -3.5\text{E}5 & -3.5\text{E}5 & 0 \\ 0 & 0 & 0 & 0 & 0 & -3.5\text{E}5 & 6.6\text{E}6 & 0 & 2.5\text{E}6 \\ 0 & 0 & 0 & 0 & 0 & -3.5\text{E}5 & 0 & 6.6\text{E}6 & -2.5\text{E}6 \\ 0 & 0 & 0 & 0 & 0 & 0 & 2.5\text{E}6 & -2.5\text{E}6 & 3.5\text{E}7 \end{bmatrix} \tag{21}$$

$$\vec{F}_{act} = \begin{bmatrix} -1.0 & 0 & 0 & 0 & 0 \\ 1.7 & 1 & 0 & 0 & 0 \\ 0 & -5.0\text{E}-1 & 0 & 0 & 0 \\ 0 & -5.0\text{E}-1 & 0 & 0 & 0 \\ 0 & 0 & 1 & 0 & 0 \\ 0 & 0 & 0 & -1 & 0 \\ 0 & 0 & 0 & 5.0\text{E}-1 & 7.1\text{E}-2 \\ 0 & 0 & 0 & 5.0\text{E}-1 & -7.1\text{E}-2 \\ 0 & 0 & 0 & 0 & 1 \end{bmatrix} \tag{22}$$

$$\vec{F}_{dist} = \begin{bmatrix} 0 & 0 & 0 & 0 & 8\text{E}4 & 1.8\text{E}4 & 8\text{E}4 & 1.8\text{E}4 & -2.8\text{E}4 & 0 & 0 & 0 & 0 & 0 \\ 0 & 0 & 0 & 0 & -1.2\text{E}5 & -2.8\text{E}4 & -1.2\text{E}5 & -2.8\text{E}4 & 0 & -5.8\text{E}4 & 0 & 0 & 0 & 0 \\ 2.1\text{E}6 & 2.3\text{E}5 & 0 & 0 & -1.5\text{E}5 & 0 & 0 & 0 & 0 & 0 & 0 & 0 & 0 & 0 \\ 0 & 0 & 2.1\text{E}6 & 2.3\text{E}5 & 0 & 0 & -1.5\text{E}5 & 0 & 0 & 0 & 0 & 0 & 0 & 0 \\ 0 & 0 & 0 & 0 & 5.6\text{E}5 & 1.2\text{E}5 & -5.6\text{E}5 & -1.2\text{E}5 & 0 & 0 & 0 & 0 & 0 & 0 \\ 0 & 0 & 0 & 0 & 0 & 0 & 0 & 0 & 0 & 0 & 0 & 0 & 0 & 0 \\ 0 & 0 & 0 & 0 & 0 & 0 & 0 & 0 & 0 & 0 & 6.3\text{E}6 & 3.3\text{E}5 & 0 & 0 \\ 0 & 0 & 0 & 0 & 0 & 0 & 0 & 0 & 0 & 0 & 0 & 0 & 6.3\text{E}6 & 3.3\text{E}5 \\ 0 & 0 & 0 & 0 & 0 & 0 & 0 & 0 & 0 & 0 & 0 & 0 & 0 & 0 \end{bmatrix} \tag{23}$$

References

[1] *DB presents study on expansion of high-speed rail in Europe*. 2024. URL: https://www.deutschebahn.com/en/presse/press_releases/DB-presents-study-on-expansion-of-high-speed-rail-in-Europe-10878406 (visited on 01/09/2024).

[2] Bin Fu et al. "Active suspension in railway vehicles: a literature survey". In: *Railway Engineering Science* 28.1 (2020), pp. 3–35. ISSN: 2662-4745. DOI: 10.1007/s40534-020-00207-w.

[3] Rickard Persson, Roger M. Goodall, and Kimiaki Sasaki. "Carbody tilting – technologies and benefits". In: *Vehicle System Dynamics* 47.8 (2009), pp. 949–981. ISSN: 0042-3114. DOI: 10.1080/00423110903082234.

[4] D. H. Allen. "Active bumpstop hold-off device". In: *Proc IMechE Conference Railtech*. Vol. 94. 1994.

[5] D. Karnopp. "Active and Semi-Active Vibration Isolation". In: *Journal of Vibration and Acoustics* 117.B (1995), pp. 177–185. ISSN: 1048-9002. DOI: 10.1115/1.2838660.

[6] Anneli Orvnäs, Sebastian Stichel, and Rickard Persson. "Active lateral secondary suspension with H∞ control to improve ride comfort: simulations on a full-scale model". In: *Vehicle System Dynamics* 49.9 (2011), pp. 1409–1422. ISSN: 0042-3114. DOI: 10.1080/00423114.2010.527011.

[7] Patience E. Orukpe et al. "Model predictive control based on mixed H2 /H∞ control approach for active vibration control of railway vehicles". In: *Vehicle System Dynamics* 46.sup1 (2008), pp. 151–160. ISSN: 0042-3114. DOI: 10.1080/00423110701882371.

[8] Alexander Posseckert and Daniel Lüdicke. "Ride Comfort Improvements on Disturbed Railroads Using Model Predictive Control". In: *Vehicles* 5.4 (2023), pp. 1353–1366. DOI: 10.3390/vehicles5040074.

[9] *Future Railway Mobile Communication System: User Requirements Specification*. 2024. URL: https://uic.org/spip.php?action=telecharger&arg=3054 (visited on 01/15/2024).

[10] J. Winter. "Novel Rail Vehicle Concepts for a High Speed Train: The Next Generation Train". In: *Proceedings of the First International Conference on Railway Technology: Research, Development and Maintenance*. Ed. by J. Pombo. Civil-Comp Proceedings. Civil-Comp PressStirlingshire, UK, 2012. DOI: 10.4203/ccp.98.22.

[11] Andreas Heckmann et al. "A Research Facility for the Next Generation Train Running Gear in True Scale". In: *Advances in Dynamics of Vehicles on Roads and Tracks II*. Ed. by Anna Orlova and David Cole. Vol. 9. Lecture Notes in Mechanical Engineering. Cham: Springer International Publishing, 2022, pp. 18–27. ISBN: 978-3-031-07304-5. DOI: 10.1007/978-3-031-07305-2_3.

[12] *DIN EN 12299:2009-08, Bahnanwendungen - Fahrkomfort für Fahrgäste - Messung und Auswertung; Deutsche Fassung EN 12299:2009*. Tech. rep. Berlin: Deutsches Institut für Normung, 2009. DOI: 10.31030/1522503.

[13] Andreas Heckmann, Alexander Keck, and Gustav Grether. "Active Guidance of a Railway Running Gear with Independently Rotating Wheels". In: *2020 IEEE Vehicle Power and Propulsion Conference (VPPC)*. Piscataway, NJ: IEEE, 2020, pp. 1–5. ISBN: 978-1-7281-8959-8. DOI: 10.1109/VPPC49601.2020.9330922.

[14] A. Posseckert and D. Lüdicke. "Ride comfort improvements in switches using active secondary suspension with preview". In: *Proceedings of the Fifth International Conference on Railway Technology: Research, Development and Maintenance*. Ed. by J. Pombo. Civil-Comp Conferences. Civil-Comp PressEdinburgh, United Kingdom, 2023, pp. 1–6. DOI: 10.4203/ccc.1.34.2.

[15] Matthew J. Benacquista and Joseph D. Romano. *Classical Mechanics*. 1st ed. 2018. Undergraduate Lecture Notes in Physics. Cham: Springer International Publishing and Imprint: Springer, 2018. ISBN: 9783319687803.

[16] C. Schmid and L. T. Biegler. "Quadratic programming methods for reduced hessian SQP". In: *Computers & Chemical Engineering* 18.9 (1994), pp. 817–832. ISSN: 00981354. DOI: 10.1016/0098-1354(94)E0001-4.

[17] Francesco Borrelli, Alberto Bemporad, and Manfred Morari. *Predictive control for linear and hybrid systems*. Cambridge, New York, and Port Melbourne: Cambridge University Press, 2017. ISBN: 9781107016880.

[18] *DIN EN 14363:2022-10, Bahnanwendungen - Versuche und Simulationen für die Zulassung der fahrtechnischen Eigenschaften von Eisenbahnfahrzeugen - Fahrverhalten und stationäre Versuche; Deutsche Fassung EN 14363:2016 + A1:2018 + A2:2022*. Tech. rep. Berlin: Deutsches Institut für Normung e.V., 2022. DOI: 10.31030/3376515.